# An Experimental Study of the Pyrolysis and the Oxidation of Ethylene Glycol and Propylene Glycol in a Jet-Stirred Reactor

Suphaporn Arunthanayothin, Olivier Herbinet, Frédérique Battin-Leclerc

# An experimental study of the pyrolysis and the oxidation of ethylene glycol and propylene glycol in a jet-stirred reactor

Suphaporn Arunthanayothin[a], Olivier Herbinet[a,*], Frédérique Battin-Leclerc[a]

[a] Laboratoire Réactions et Génie des Procédés, CNRS, Université de Lorraine, ENSIC, 1 rue Grandville, 54000 Nancy Cedex, France

* Corresponding author's email address: olivier.herbinet@univ-lorraine.fr (O. Herbinet).

Published in Energy & Fuel, 2022, 36, 22, 13678–13687

**Abstract**

This work investigates experimentally the pyrolysis and oxidation of ethylene glycol (EG) and propylene glycol (PG), two candidate molecules as model surrogates of biomass-based pyrolysis oils, the structure of which is included in sugars. This paper reports the first experiments with these high boiling point (~470 K for EG, 461 K for PG) di-oxygenated molecules performed in a fused silica jet-stirred reactor. Pyrolysis and oxidation experiments are carried out for 1% fuel/He mixture over a temperature range T=600-1200 K. EG oxidation experiments are performed at three equivalence ratios (φ = 0.5, 1.0 and 2.0), while those for PG were only performed under stoichiometric condition. The residence time is 2 seconds and the pressure is quasi atmospheric (107 kPa). Experimental data clearly show differences in the reactivity of both fuels. Results for EG are compared to simulations using a literature detailed kinetic model and indicate significant deviations and the need to further refine the diol chemistry in detailed kinetic models. Rate-of-production and sensitivity analyses point out important pathways that should be further investigated for a better understanding of glycol combustion chemistry, like concerted decomposition reactions of the fuel and the consideration of ethenol instead of its analog aldehyde, acetaldehyde.

**Keywords:** ethylene glycol, propylene glycol, jet-stirred reactor, pyrolysis, oxidation, bio-oil.

## 1. Introduction

With increasing concerns about climate change and the rapid depletion of fossil fuels, industries and academia are looking for alternative energy sources. In the EU, the target of energy consumption from renewable sources by 2030 is set at least to 32%.[1] Fast biomass pyrolysis is one of the alternatives to obtain high yields of bio-oils, which can be upgraded to valuable fuels for transport and chemicals for industry.[2] Moreover, alcohols have been widely used as alternatives fuels or fuel additives (i.e. bioethanol, biobutanol) because they can inhibit the formation of soot and polyaromatic hydrocarbons (PAHs).[3–6] The diol molecules, ethylene glycol (EG) and propylene glycol (PG, also named 1,2-propanediol), gained attention amongst components of biofuels due to their similarity with biomass pyrolysis oil in chemical composition and physical properties.[7,8] The EG molecule is also a substructure of sugars, as well as a major industrial chemical used in the production of polyester fibers and films, antifreeze, refrigerant and vitrification formulations. PG has many industrial or agro-pharmaceutical uses, at low doses as a food additive and recently in electronic cigarettes. Therefore, the study of PG oxidation can help identifying pollutants formed during smoking of this type of cigarettes is case of malfunction.

A bibliographical review shows a lack of available kinetic studies about the pyrolysis and the oxidation of diols, even for EG despite its particularly simple and symmetric structure (HO—$CH_2$—$CH_2$—OH). The lack of experimental data is likely related to the difficulties in handling these fuels. The structures of EG, of PG ($CH_3$—CH(—OH)—$CH_2$—OH) and of propanol ($CH_3$—$CH_2$—$CH_2$—OH) are close; however, the boiling point rises from 370 K for propanol up to 461 K for PG and 470 for EG due to higher intermolecular forces in diols due to hydrogen bonds. This also results in higher viscosity. A first reaction mechanism of EG oxidation was proposed in 2011 by Hafner *et al.*[9] based on a $C_1$–$C_4$ mechanism[10] enhanced by reactions of ethanol taken from Marinov[11] and on EG reaction rate constants estimated using analogy methods. In 2012, Ye *et al.*[12,13] investigated theoretically the unimolecular decomposition of EG, PG, 1,3-propanediol and glycerol computing the rate constants of the main reaction channels by ab initio calculations. In 2017, Kathrotia *et al.*[8] performed a first experimental and modeling study of EG oxidation. These data included measurements of ignition delay times using a shock tube over the temperature range of 800–1500 K at 16 bar and of species profiles measured in a flow reactor over the range 700–1200 K. Their EG model based on that published by Hafner *et al.*[9,14] reasonably simulated their experimental data. To the authors knowledge, there is neither experimental study

nor kinetic study concerning the combustion of PG. The gas-phase pyrolysis of PG was investigated by Laino et al.[15] using a pyroprobe device operating at 800 K and coupled to gas chromatography for product analysis. They observed significant amounts of methyloxirane, propanal and acetone. Other products were acetaldehyde, allyl alcohol and hydroxyacetone. Quantum calculations performed by these authors suggest that PG undergoes a dehydration reaction to methyloxirane, which then isomerizes to ketone or propanal. They identified another dehydration pathway leading to allyl alcohol. Very recently, PG pyrolysis was investigated by Al Gemayel in a quartz tube at temperatures ranging from 353.15 to 945.15 K, at a mean residence time of 1.6 s.[16] HPLC was used for species detection and detected reaction products were: propanal, acetone, acetaldehyde, formaldehyde, glyoxal and methylglyoxal.

Since investigations on EG and PG pyrolysis and oxidation would help better understanding the decomposition of these molecules and the pollutants, which can be yielded during their combustion, the present work aims at investigating experimentally these reactions in a Jet-Stirred Reactor (JSR) under quasi atmospheric pressure. A detailed analysis of reaction products and intermediates is performed and, in the case of EG, the results are interpreted using the kinetic model of Kathrotia et al..[8] To the knowledge of the authors this is the most recent model with including detailed oxidation and pyrolysis chemistry for ethylene glycol, and validated against speciation (flow reactor) and ignition delay time data.

## 2. JSR experimental set-up and conditions

Experiments on the pyrolysis and the oxidation of EG have been carried out covering stoichiometric, fuel-rich and fuel lean conditions; those about PG have only been performed under pyrolysis and stoichiometric oxidation conditions. This section describes the apparatus and the analytical methods used to perform these experiments.

JSRs are usually used in gas-phase kinetic studies and the setup of the present work was already described in details;[17–19] only a brief description is provided here. Experiments were carried out in a fused silica JSR (85 $cm^3$), a type of continuous stirred-tank reactor usually operated under steady state. It consists of a spherical vessel with injection of the mixture through four nozzles located at the center of the reactor, creating high turbulence resulting in homogeneity in temperature and composition. As a result, the JSR can be modeled

as a perfectly stirred reactor. Inconel resistances were used to heat the reactor and its preheating zone, and the reaction temperature was measured with a K-type thermocouple located in a glass finger close to the center of the reactor (uncertainty of ±5K).

As shown in Table 1, six sets of EG and PG experiments were performed under conditions close to atmospheric pressure (0.107MPa), at a residence time (τ) of about 2 s, with helium as carrier gas and an initial fuel mole fraction of 0.01. The pyrolysis and oxidation of EG and PG were performed at temperatures ranging from 600 to 1100 K.

**Table 1:** Summary of JSR experimental conditions used in the EG and PG studies.

| Set | T [K] | P [MPa] | τ [s] | ϕ[a] | Inlet mole fraction (%) | | | |
|---|---|---|---|---|---|---|---|---|
| | | | | | EG | PG | $O_2$ | He |
| 1 | 650-1100 | 0.107 | 2 | ∞ | 1.00 | - | 0.00 | 99.00 |
| 2 | 600-1075 | | | 0.5 | 1.00 | - | 5.00 | 94.00 |
| 3 | 600-1075 | | | 1 | 1.00 | - | 2.50 | 96.50 |
| 4 | 600-1075 | | | 2 | 1.00 | - | 1.25 | 97.75 |
| 5 | 650-1100 | | | ∞ | - | 1.00 | 0.00 | 99.00 |
| 6 | 600-1200 | | | 1 | - | 1.00 | 4.00 | 95.00 |

[a] Equivalence ratios (ϕ) of EG and PG were respectively defined by the following stoichiometric equations: $C_2H_6O_2 + 2.5\ O_2 = 2\ CO_2 + 3\ H_2O$ and $C_3H_8O_2 + 4\ O_2 = 3\ CO_2 + 4\ H_2O$.

Mass flow controllers were used for reactor feeding (relative uncertainty of ±0.5% in flow). A liquid Coriolis flow controller was used to control the flow of diol mixed with helium to form an aerosol and passed through an evaporator before being mixed with oxygen prior to entering the reactor. The temperature of the evaporator (473K) was set at above the EG boiling temperature to avoid fuel condensation. Helium and oxygen were provided by Messer (purity of 99.999%). EG and PG were provided by Merck (previously Sigma-Aldrich) with a purity of 99.8% and 99.5%, respectively. Note that PG is chiral because of the central carbon atom and that the product provided by Merck is probably a racemic mixture (this information was not available). As expected because of similar physical properties, only one peak was observed in chromatograms for PG.

To avoid condensation, the reactants and reaction products leaving the reactors were transported by a heated transfer line maintained at 393 K to two gas chromatographs (GCs). The first GC equipped with a Carbosphere-packed column, a flame ionization detector (FID) and a thermal conductivity detector (TCD) was used to quantify lightweight species using argon as carrier gas for $H_2$ (only quantified for pyrolysis of EG and

PG and for oxidation of PG) and He as carrier gas for the detection of other species (like $O_2$). The second GC fitted with a Q-Bond capillary column and a FID preceded by a methanizer was used for the quantification of compounds containing from one to three carbon atoms. The methanizer (nickel catalyst for hydrogenation) allows an easier detection of species, like CO, $CO_2$, formaldehyde, and acetaldehyde. Moreover, due to the condensation of outlet heavy species (e.g., EG, PG, formic acid) in the transfer line to GCs, a trap maintained at liquid nitrogen temperature was used in separate experiments to perform offline analyses. The trap was connected to the outlet of the reactor and the outlet flow condensed due to the low temperature during a period of 15 minutes. The sample was then mixed with an internal standard (100 µL of *n*-octane) and a solvent (ethanol), allowing for the dilution of the liquefied sample. It is possible that condensation and physical adsorption occurred on some surfaces in the manifolds (cold points, valve, gums). This could affect the quality of the results. The sample was then injected to a GC fitted with an automatic liquid sampler, a Q-Bond capillary column with FID and mass spectrometry (GC-MS) detections. Note that experiments with and without trapping had to be performed separately. The calibration of EG and PG was made by preparing mixtures of known compositions. Formic acid mole fractions were calculated from the FID signal using *n*-octane as internal standard (offline analysis). The relationship between formic acid and *n*-octane mole fractions was deduced from an external calibration performed by injecting mixtures of both species with known amounts. The comparison of response factors of both species confirmed that the FID is not very sensitive to formic acid, as it could be expected as this species is highly oxidized. For small species, such as $H_2$, CO, $CO_2$, $O_2$, and $CH_4$, GC calibrations were performed using gaseous standards provided by Messer and Air Liquide. Other species detected with the FID were calibrated using the effective carbon number (ECN) method. Relative uncertainties in mole fractions of species detected by GCs and calibrated using gaseous standards provided by Messer and Air Liquide were estimated to ±5%. The relative uncertainty in the mole fractions of ethylene glycol was estimated to ±10% due to the difficulties in handling this species (probably due to adsorption phenomena). Relative uncertainties in mole fractions of species calibrated using the ECN methods were estimated to ±10%.

The carbon balance for the four EG experiments (Phi = ∞, 0.5, 1, and 2) are shown in Figure 1a; due to uncertainties in species mole fractions, the carbon balance can be slightly higher than 100%. A carbon balance below to 80% was observed from 875 to 1025 K during EG pyrolysis and from 725 to 925 K during EG oxidation. This indicates species that were not detected in these temperature ranges.

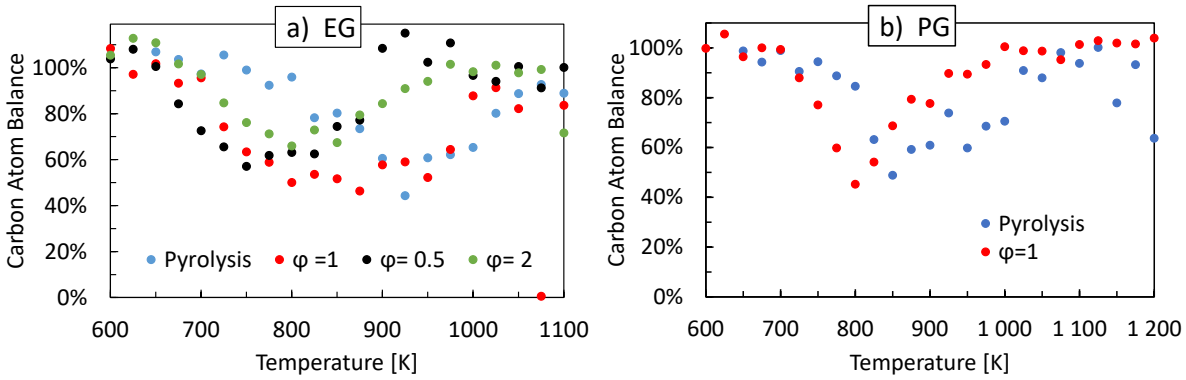


Figure 1: Carbon atom balances for the experimental results of EG (a) and PG (b).

The carbon balances calculated for the experimental data of PG ($\varphi$ = 1 and $\infty$) are displayed in Figure 1b. Carbon balances for PG oxidation are globally better than those of PG pyrolysis. However, a carbon balance below 80% was observed over the temperature ranges of 750-900K during oxidation and of 825-1000 K during pyrolysis, also indicating species that were not detected (for ethylene glycol, this could be species like hydroxy acetaldehyde and glyoxal which are intermediates involved in the chemistry of the literature model of Kathrotia et al.[8] and which were not detected in the present work). This non-detection of these species might be due to condensation in the transfer line, which is emphasized in the case of glycols due to the probable formation of low-volatility intermediates with several oxygen atoms.

## 3. Description of the obtained experimental results

This section presents the experimental data obtained for EG and PG pyrolysis and oxidation. PG and EG molecules are similar with the same functional groups (diol) containing two hydroxyl groups (-OH groups) but different in the number of carbons.

### 3.1. EG and PG pyrolysis

A comparison of the temperature evolutions of the species mole fractions measured during of the pyrolysis of EG and PG is presented in Figure 2. The temperatures of reactivity onset of PG and EG are ~775 K and 825 K, respectively, indicating that EG is less reactive than PG. Reaction products detected during both the PG and EG pyrolysis studies are $H_2$, methane, carbon monoxide, carbon dioxide, ethylene, ethane, acetaldehyde, propene and acetone. Acetylene, with large mole fractions, is only produced from PG. The CO and methane profiles during the pyrolysis of the two fuels are quite similar, with mole fractions increasing over the whole studied temperature range. However, during PG pyrolysis, more acetone ($CH_3COCH_3$), acetaldehyde ($CH_3CHO$), propylene and ethylene are formed than during EG pyrolysis. The formation of large mole fractions of acetone with PG can be explained by the reaction of dehydration PG $\rightarrow CH_3COCH_3 + H_2O$. Acetaldehyde formation is observed for both fuels, probably via dehydration from the fuel for EG and via a more complex path for PG. The significant amounts of propene detected in PG experiments also suggests that some pathways lead to the loss of both hydroxy groups. The formation of $C_2$ species for PG indicates that decomposition pathways play an important role in the pyrolysis chemistry of this fuel. In contrast to PG, ethane formation seems to be favored in the case of EG, which implies the removal of the two oxygen atoms; this cannot be explained by simple steps. During the pyrolysis of PG, ethanol is produced at a lower temperature (675 K) than in the case of EG (800 K). However, the maximum ethanol produced for the two cases is similar (~ 30 ppm).

Comparisons with literature experimental studies about PG pyrolysis[15,16] highlight significant differences in the nature of reactions products. The present study suggests that the main PG dehydration pathway leads directly to acetone (as methyloxirane and propanal were not observed), whereas the data obtained by Laino et al.[15] suggests that PG dehydration leads to methyloxirane, which in turn isomerizes to propanal and acetone. Al Gemaye et al.[16] observed both acetone and propanal, but not methyloxirane (because

their analytical method was only specific to carbonyl species). Methyloxirane and propanal are common oxidation products that were easily detected in previous studies by our group[19,20] and there is no reason for not detecting them in the present study if formed. The two PG pyrolysis literature studies were performed under different conditions than the present one (especially the hydrodynamics due to different reactor types), which can explain these differences in the product selectivity. Also, the use of glass fiber filters in the literature studies might enhance wall reactions if the temperature is still high in this part of the setup.

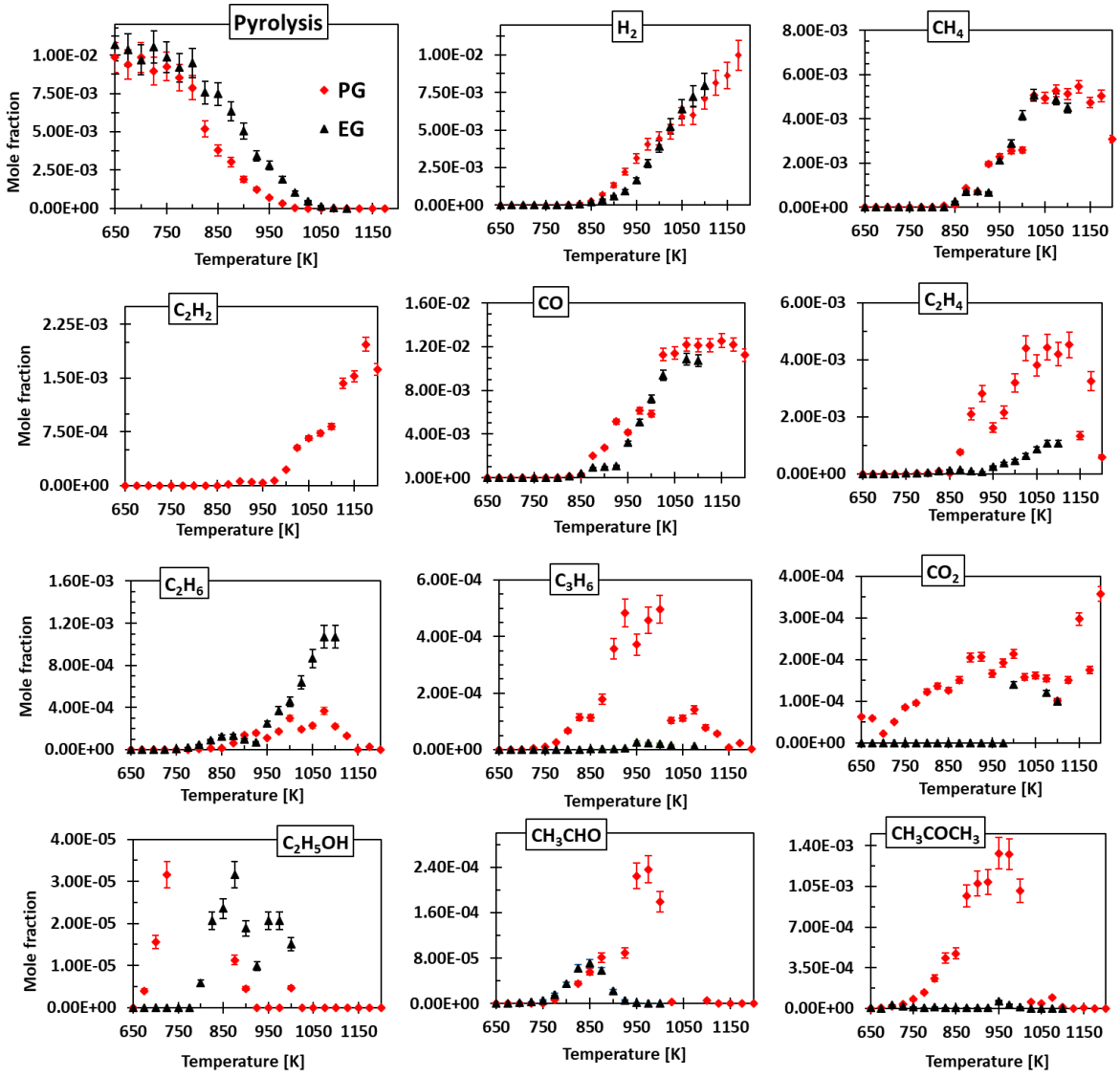


Figure 2: Mole fractions of reactants and main reaction products during the pyrolysis of PG and EG over the temperature range 650-1200 K in the JSR ($x_{fuel}^{inlet}$= 1%, P = 0.107 MPa and τ = 2 s). Red diamond symbols: PG experiments. Black triangle symbols: EG experiments.

### 3.2. EG and PG oxidation

A comparison of the experimental results of PG and EG oxidation (φ = 1) is displayed in Figure 3. This figure shows that PG and EG have similar evolution of the reactivity with temperature, but that EG seems to be slightly more reactive than PG: EG consumption begins at 675 K, while PG is only consumed from 725 K; i.e. about 100 K lower than during pyrolysis, well indicating that the presence of oxygen enhances the fuel reactivity.

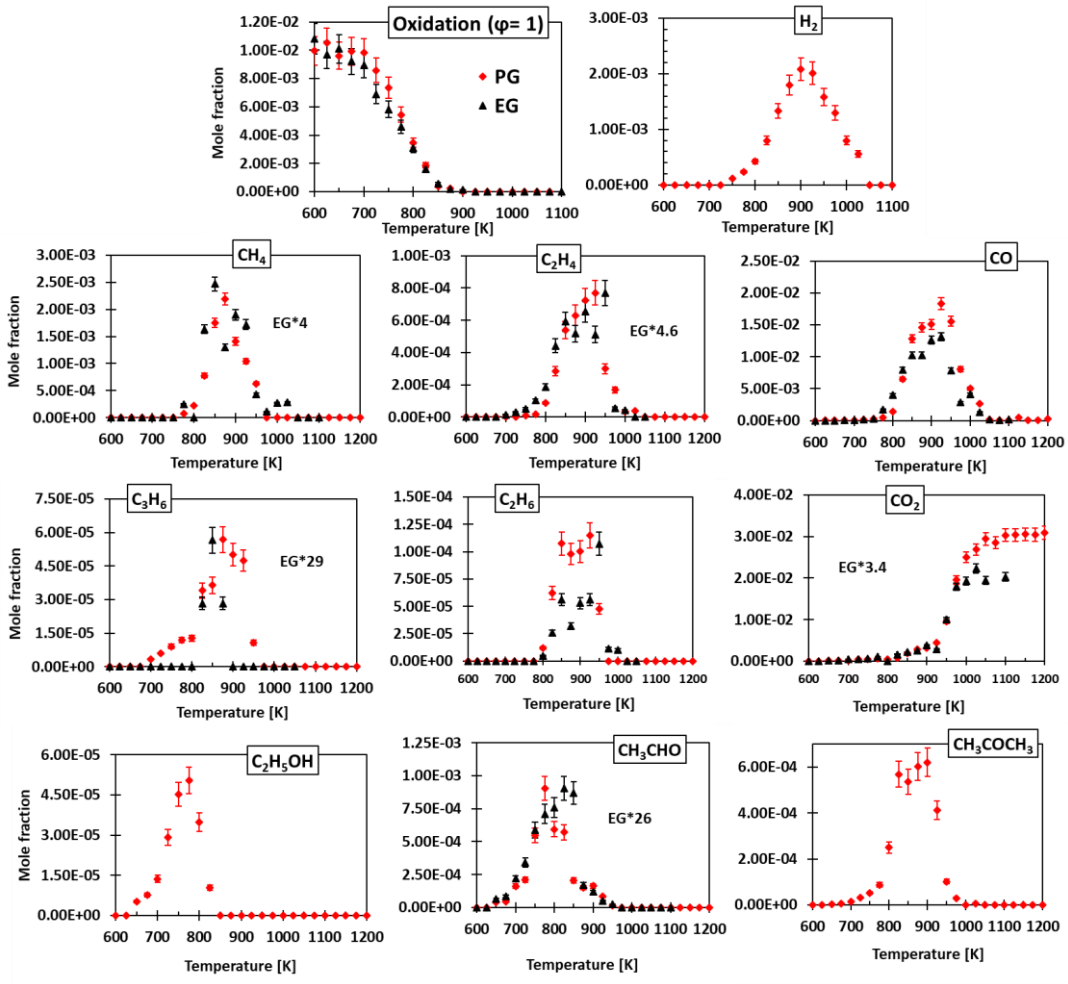


Figure 3: Mole fractions of reactants and main reaction products during the oxidation (φ = 1) of PG and EG over the temperature range 600-1200 K in the JSR ($x_{fuel}^{inlet}$ = 1%, P = 0.107 MPa and τ = 2 s). Red diamond symbols: PG experiments. Black triangle symbols: EG experiments.

Figure 4 shows the experimental results for EG oxidation for the three investigated equivalence ratios, 0.5, 1, 2 and indicates a slight promoting effect of decreasing ϕ. The consumption of $O_2$ begins after that of ethylene glycol which means that fuel decomposition reaction is dominant at low temperature. $O_2$ is consumed from ~800 K for three mixture conditions, but $O_2$ consumption for φ = 2.0 is faster than the other mixtures.

The conversion of oxygen is slow at low temperatures but is entirely completed at high temperatures except for $\phi = 0.5$, for which $O_2$ was not totally consumed and remained at ~2000 ppm. Oxygen measurements during PG oxidation could not be exploited due to unexpected and unexplained scattering of GC areas ($O_2$ is the only species for which this scattering was observed).

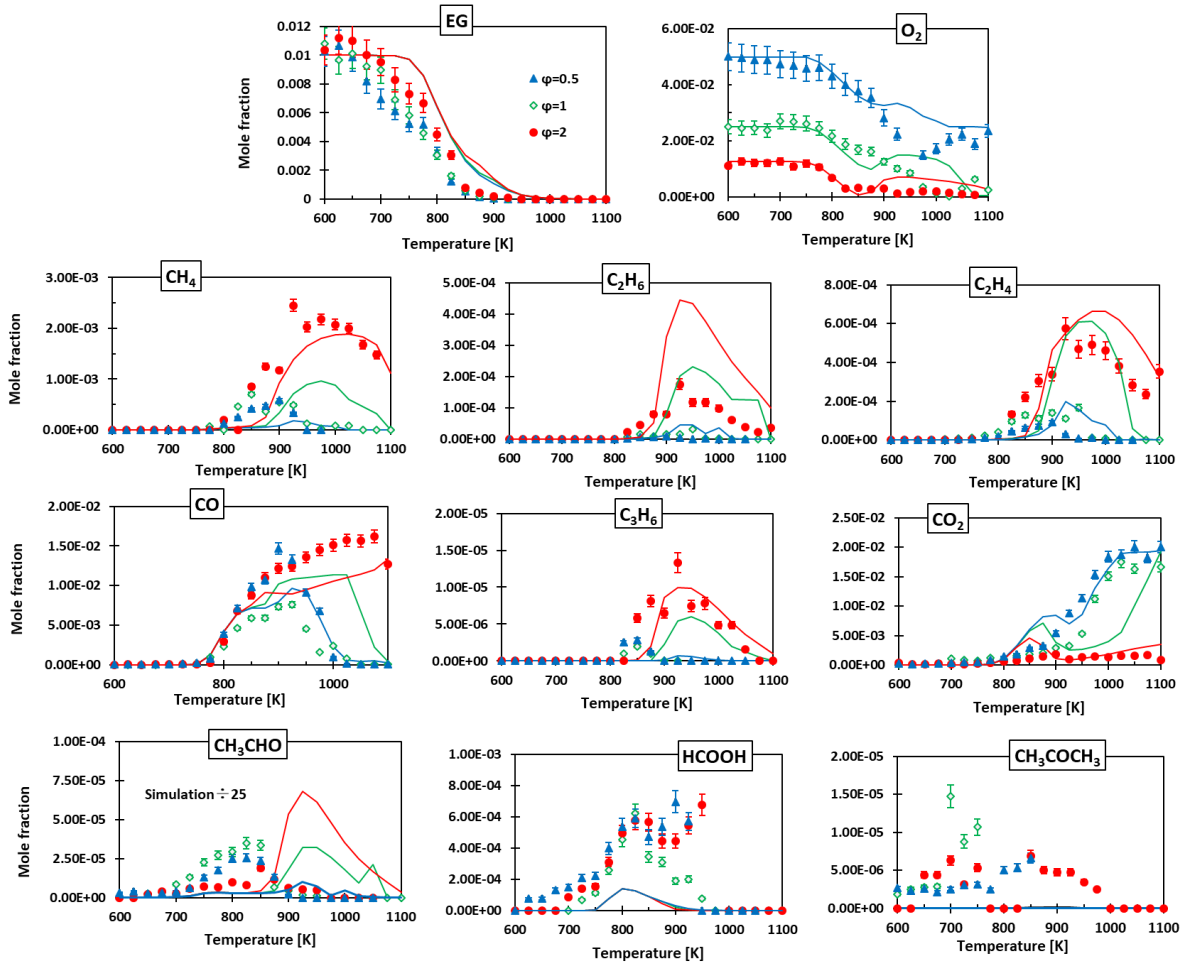


Figure 4: Mole fractions of reactants and main reaction products during the oxidation of 10000 ppm EG in the JSR ($\varphi = 0.5$, 1 and 2, P = 0.107 MPa and $\tau = 2$ s). Symbols: experiments (full triangles: $\varphi = 0.5$, empty diamonds: $\varphi = 1$, full circles: $\varphi = 2$). Lines: data computed with the literature model of Kathrotia et al.[8]

Except $CO_2$, all the quantified products are intermediates with their mole fractions going through a maximum. Figure 5a displays the reaction product selectivity analysis for EG pyrolysis and oxidation ($\varphi = 0.5$, 1, 2) and Figure 5b presents the reaction product selectivity analysis for PG pyrolysis and oxidation ($\varphi = 1$).All these analyses were performed at 850 K corresponding to an EG conversions about 25 % and 93% and a PG conversions about 62% and 96%, under pyrolysis and oxidation conditions, respectively.

Reaction products detected during the oxidation experiments are the same as those detected during pyrolysis, except for hydrogen, only observed for PG oxidation. A notable formation of ethanol is only

observed during the pyrolysis of both diols. Common reaction products detected during EG and PG oxidation experiments are carbon monoxide, carbon dioxide, methane, ethylene, ethane, acetaldehyde, propene and acetone. Formic acid was only observed during EG oxidation. The main PG pyrolysis products (> 10%) are acetone, 2-propenal (acrolein), CO and $H_2$. The presence of $O_2$ in the PG experiments promotes the formation of $CO_2$ and CO but reduces that of $H_2$. During oxidation, as is shown in Figure 5, except for CO, which is by far the major product (selectivity above 60%), much larger mole fractions of the quantified products are obtained for PG than for EG oxidation. This is because PG molecule is larger than EG one, leading to more decomposition products, especially hydrocarbon ones. A specificity of PG is the large amount of acetone detected in experiments, probably due to a concerted water elimination pathway (as for EG, see discussion in the next section). If it is the case, the absence of propanal amongst reaction products would indicate that the water elimination is highly disfavored when the OH group of the central carbon atom is eliminated.

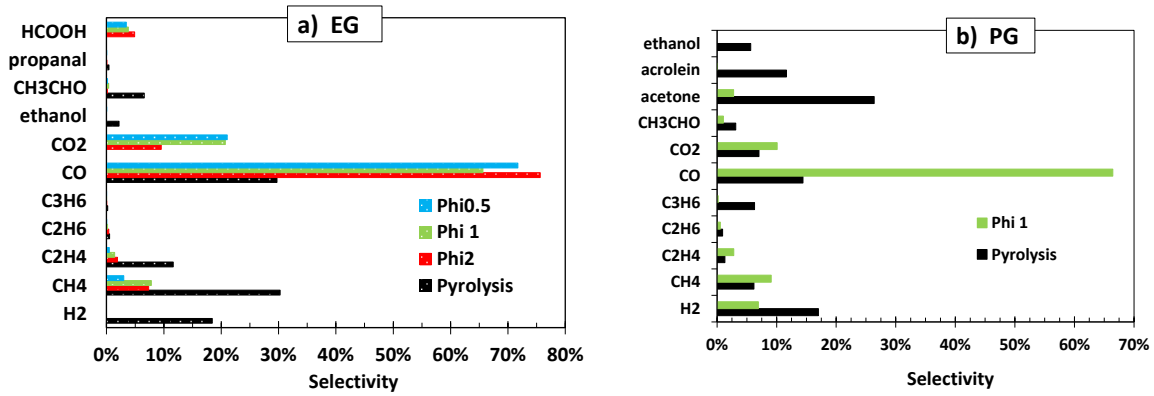


Figure 5: Reaction product selectivity analysis for EG (a) and PG (b) pyrolysis and oxidation at 850 K.

## 4. Comparison between experimental and simulated results

In this section, the EG experimental data are compared to simulations using the kinetic model of Kathrotia et al..[8] To the best of our knowledge, no model is available for PG pyrolysis and oxidation, so no comparison could be performed for this species. The primary reactions of EG in the model of Kathrotia et al.[8] include the unimolecular initiation by C-C bond breaking (C-H bond breaking was not considered), the bimolecular initiation with $O_2$, and several concerted reactions leading to methanol and formaldehyde, acetaldehyde and water, hydroxy acetaldehyde and hydrogen. It also includes fuel H-atom abstractions involving, O and H atoms, as well as OH, $HO_2$, HCO and HCCO radicals. These H-abstractions yield two possible fuel radicals, ($CH_2OH\dot{C}HOH$) and HOCH2CH2CO$\dot{}$). Reaction consuming these two these two fuel

radicals are decomposition through C-C- and C-H β-scission, oxidation (H-atom abstraction reaction with $O_2$), and termination by disproportionation with radical species like H, O and OH).

### 4.1. Simulations results

Figure 6 compares the mole fractions of reactants and main products predicted using the model with the pyrolysis data described in part 2.

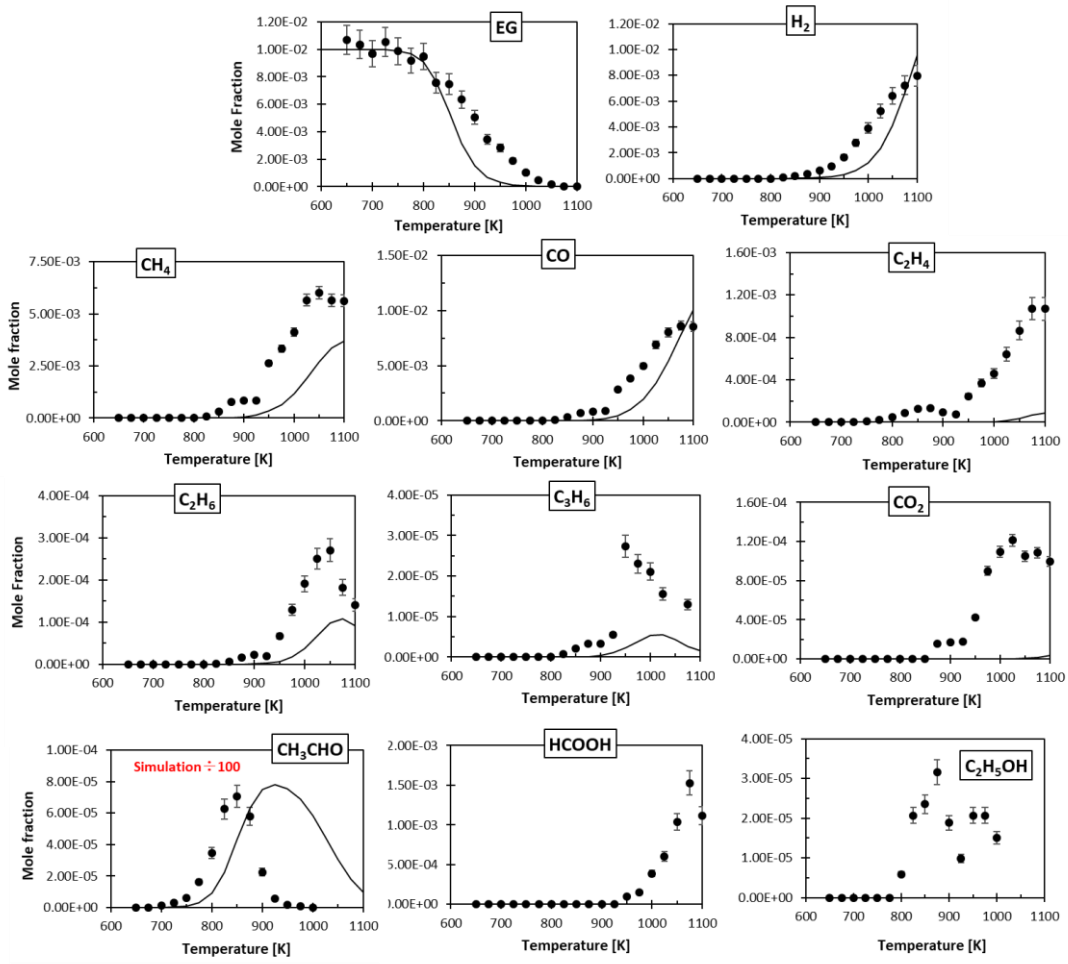


Figure 6: Mole fractions of reactants and main reaction products during the pyrolysis of EG over the temperature range 650-1100 K in the JSR (P = 0.107 MPa and τ = 2 s). Symbols: experiments. Lines: data computed with the literature model of Kathrotia et al.[8].

As is shown in Figure 6, the temperature of the reactivity onset of EG pyrolysis around 800 K is well predicted by the model, however the EG conversion is underestimated for T > 850 K. The model also slightly underpredicts the evolution of the mole fraction of hydrogen, carbon monoxide, and methane, the major experimental products, which are formed from 875 K, with a shift of 100 K between the experimental and computed data for $CH_4$ between 950 and 1100 K. The mole fractions of carbon dioxide, ethane and ethylene, formed in lower amounts, are more significantly underestimated, while those of acetaldehyde are over-

predicted by a factor of about 100. In addition, there is a significant shift between the experimental and computed data for acetaldehyde profile (50 K). Acetaldehyde is formed at lower temperatures in experiments than in simulations. The mole fractions of ethanol and propene remain low (less than 70 ppm) and their mole fractions are underestimated.

The comparison of model predictions and experimental measurements for the oxidation of EG for three equivalence ratios φ = 0.5, 1.0 and 2.0, are displayed in Figure 4. The simulated fuel consumption profiles are very little influenced by the equivalence ratio and the three simulated conversion curves are almost superimposed. Temperature shifts between the experimental and computed data are observed for EG conversion. EG consumption is rather correctly predicted by the model for φ = 2.0 case, even if a shift of 25 K between the experimental and computed data is observed. For the leanest cases (φ = 0.5 and 1), larger temperature shifts are observed, about 80 and 60 K, respectively. Oxygen consumption is well predicted for T< 900 K at the three equivalence ratios. The formation of CO, $CO_2$, methane, ethylene and propene is reasonably predicted for φ = 2.0 with more deviations at higher temperatures. The model over-predicts acetaldehyde formation by a factor of about 25, while the experimental data indicate a very low formation of this product (i.e., 25-30 ppm). Not only acetaldehyde mole fraction is over-predicted but also a significant temperature shift between the experimental and computed data is observed. Ethane production is strongly over-predicted, especially for φ = 1.0 and 2, whereas acetone is strongly under-predicted.

### *4.2. Flow rate and sensitivity analysis*

Even if the agreement between experimental and simulated data is not perfect, this part of the paper focuses on the understanding of the chemistry involved during the pyrolysis and oxidation (φ = 1) of ethylene glycol thanks to sensitivity analyses and rate-of production analyses. This aims to give clues on the reactions needing to be further investigated.

Figure 7 presents a flow rate analysis for fuel consumption during EG pyrolysis performed at 800 K. Under pyrolysis conditions, ethylene glycol is mostly consumed through $H_2O$-elimination reaction to form acetaldehyde ($CH_3CHO$). In this channel ($CH_2OHCH_2OH=CH_3CHO+H_2O$), the OH group abstracts the H-atom from the other OH group to form $H_2O$, while one H-atom in the $CH_2O$ group migrates to the $CH_2$ group to release a $CH_3$ group (all these transformations occur in a concerted way). This channel contributes to 98% of EG consumption. Acetaldehyde is then mainly consumed through H-abstraction reactions by $CH_3$ radicals,

forming $CH_4$ and $CH_3CO$ radicals. The $CH_3CO$ radicals are the main sources of CO, the major observed product, and are regenerating $CH_3$ radicals. The second decomposition channel of the EG molecule, yielding $CH_3OH$ + $CH_2O$ (also though a concerted mechanism), contributes only to 2% of EG consumption. This reaction involves transferring an H atom of the $CH_2$ group to the other $CH_2$ group and then a C-C bond cleavage. Methanol is consumed by H-abstraction by $CH_3$, producing $CH_3O$ radicals. These radicals then decompose to give formaldehyde. HCO radicals are then produced by H-abstraction from formaldehyde and decompose also yielding CO. Note that no fuel H-abstraction is involved during pyrolysis, only decomposition channels through concerted mechanisms, which highlight the importance of this type of channels for the pyrolysis chemistry of diols.

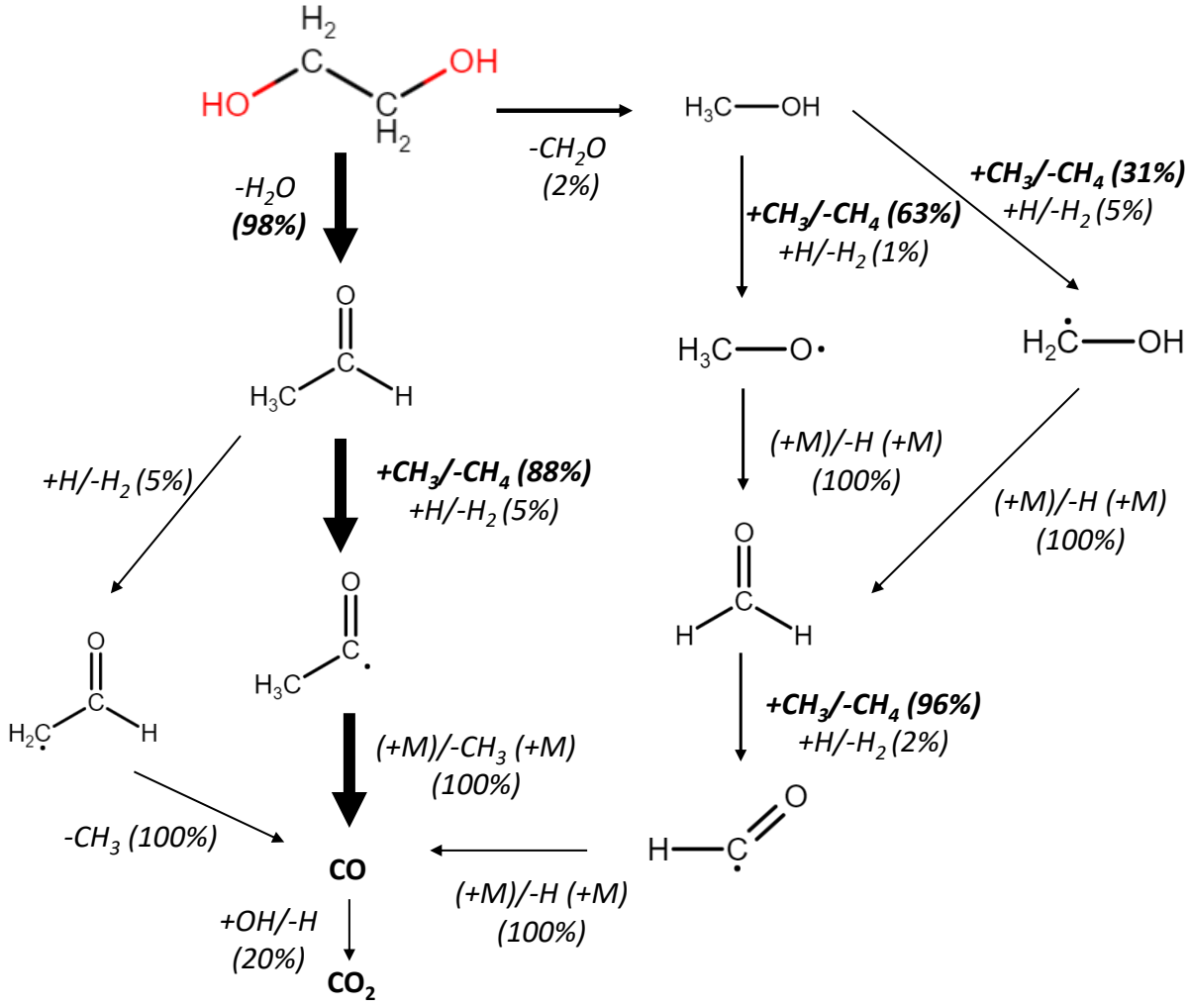


Figure 7: Consumption pathways of ethylene glycol pyrolysis at 800 K.

Figure 8 presents the flow rate analysis for fuel consumption during EG oxidation performed at 800 K. EG is mainly consumed through H-abstractions by OH and $HO_2$ radicals releasing $CH_2OH\dot{C}HOH$; this

channel contributes to 81% of EG consumption, while water elimination of EG accounts only for 19% of EG consumption. Compared to EG pyrolysis, oxygenated radicals (OH and $HO_2$), induced by the presence of oxygen in the feed, favor fuel consumption by H-abstraction reactions and lower the importance of decomposition channels through concerted mechanisms.

$CH_2OH\dot{C}HOH$ radical reacts with oxygen releasing hydroxyethanal ($CH_2OHCHO$) which is the source of ethanedial (CHOCHO, glyoxal). CHOCHO is then consumed, forming CO. Note that CHOCHO was not be detected in our experiments (probably because this species was not stable enough to accumulate or because it condensed before analysis due to its low volatility).

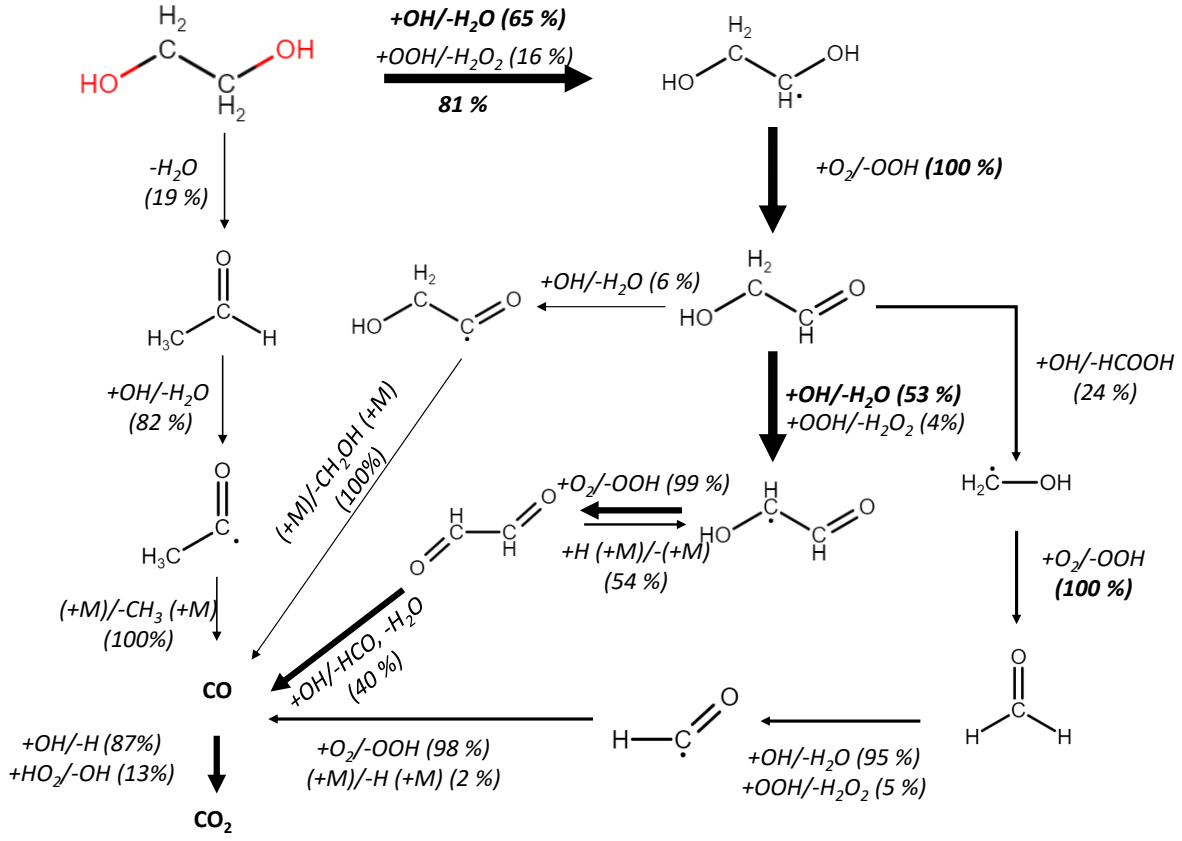


Figure 8: Consumption pathways of ethylene glycol oxidation under stoichiometric condition at 800 K.

The sensitivity analysis of EG consumption at 800 K using four different mixtures (φ = 0.5, 1.0, 2.0 and ∞) is presented in Figure 9. Under pyrolysis conditions, in line with the flow rate analysis of Figure 7, the most sensitive reaction is water elimination, releasing acetaldehyde as co-product (EG=$CH_3CHO+H_2O$). The chemistry considered for acetaldehyde in the model of Kathrotia et al.[8] is classic with initiations, H-atom abstractions and reactions of the two possible fuel radicals. The consumption of acetaldehyde cannot be held responsible for the over-estimation of this species. The rate constants of this reaction might be inaccurate, causing the acetaldehyde overprediction that is shown in Figure 6. In their theoretical study of EG unimolecular decomposition, Ye and al. [12] considered the formation of both acetaldehyde and ethenol with an energy

difference of only 0.9 kcal $mol^{-1}$. Considering that ethenol may quickly isomerize to acetaldehyde, Kathrotia et al.[8] consider the ethenol pathway but ethenol was actually replaced by acetaldehyde in the corresponding reaction. Improving diol models would probably benefit from taking into account the specific chemistry of enol species produced from diols. Further experimental and theoretical investigations on these reactions are thus highly recommended

Under oxidation conditions, the most sensitive reactions are H-abstraction reactions by OH and $HO_2$, forming $CH_2OH\dot{C}HOH$ radicals (R-CHOH), which promote fuel consumption. One of the major sources of $H_2O_2$ is from $HO_2$ radical ($HO_2+H_2O=H_2O_2+OH$ and $2HO_2=H_2O_2+O_2$), decreasing system reactivity.

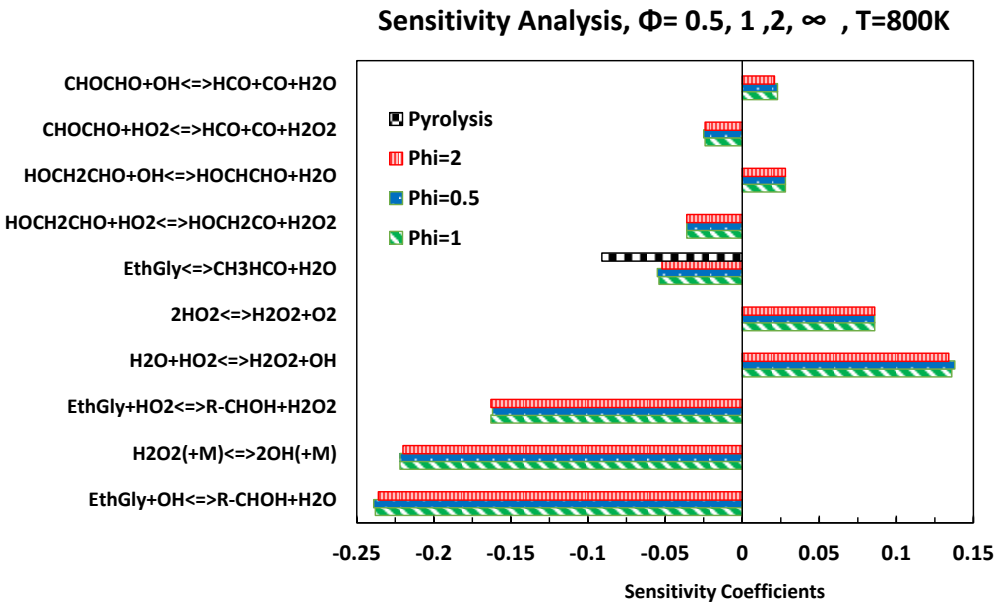


Figure 9: Sensitivity analysis of EG consumption at 800 K for the φ = 0.5, 1.0, 2.0 (65% fuel conversion) and ∞ (3% fuel conversion), P = 0.107 MPa. A negative sensitivity coefficient stands for a reaction increasing reactivity and vice versa.

## Conclusions

In this work, the pyrolysis and the oxidation of ethylene glycol and propylene glycol were experimentally investigated in a jet-stirred reactor under atmospheric pressure and high dilution (fuel mole fraction of 0.01). To the authors' best knowledge these EG and PG experimental works are the first ones performed in a JSR in the literature. The scarcity of literature data for these fuels with a simple structure could seem surprising. It is likely due to experimental difficulties specific to this class of compounds, as it was experienced in the present study. Thus, these new experiments provide an original database on the species profiles of various major products and intermediates. Comparison of the EG experimental results with simulations using a literature kinetic model showed a reasonable, but improvable, agreement for the reactivity

and for the mole fractions of major reaction products. Moreover, the EG oxidation chemistry should be further investigated because simulations for minor products, especially acetaldehyde and hydrocarbons indicate significant deviations between experimental and computed data. Solving the problem of the overestimation of acetaldehyde production (100 times more than experimental data for pyrolysis) will require deeper investigations of the specific chemistry involved in the gas phase kinetics of EG and ethenol, which should be better considered in a future kinetic model. Thus, complementary experimental data and theoretical studies are needed to improve the related rate constants and to provide more knowledge on the role of ethenol in EG oxidation. This conclusion can probably be extended to sugars and sugar polymers, the structures of which include diol patterns.

Comparison of the PG experimental results with EG results showed a difference of reactivity between these two fuels, which could help to better understand diol chemistry. These experimental data will be a basis for the development of a detailed kinetic model for PG pyrolysis and oxidation that does not exist in the literature. The structure of PG is similar to that of EG but the development of a detailed kinetic model for PG may require significant efforts to the loss of the symmetry. As for ethylene glycol, concerted molecular pathways might play an important role as suggested by the significant amount of acetone detected in experiments. Further theoretical investigations are also needed to understand why elimination involving the OH group of the central carbon atom is such disfavored as suggested by the absence of propanal.

**Supplemental material description**

An Excel file named SM1 containing jet-stirred reactor experimental data and atomic balance calculations.

**Acknowledgements**

This work has received funding from the Scientific Research National Center (CNRS) and the Reactions and Process Engineering Laboratory (LRGP).

**References**

(1) Communication from the Commission to the European Parliament and the Council: Energy Efficiency and Its Contribution to Energy Security and the 2030 Framework for Climate and Energy Policy; 2014.

(2) Hu, X.; Gholizadeh, M. Progress of the Applications of Bio-Oil. Renew. Sustain. Energy Rev. 2020, 134, 110124. https://doi.org/10.1016/j.rser.2020.110124.

(3) Ni, T.; Pinson, J. A.; Gupta, S.; Santoro, R. J. Two-Dimensional Imaging of Soot Volume Fraction by the Use of Laser-Induced Incandescence. Appl. Opt. 1995, 34 (30), 7083–7091. https://doi.org/10.1364/AO.34.007083.

(4) Kitamura, T.; Ito, T.; Senda, J.; Fujimoto, H. Extraction of the Suppression Effects of Oxygenated Fuels on Soot Formation Using a Detailed Chemical Kinetic Model. JSAE Rev. 2001, 22 (2), 139–145. https://doi.org/10.1016/S0389-4304(00)00108-9.

(5) Wu, J.; Song, K. H.; Litzinger, T.; Lee, S.-Y.; Santoro, R.; Linevsky, M.; Colket, M.; Liscinsky, D. Reduction of PAH and Soot in Premixed Ethylene–Air Flames by Addition of Ethanol. Combust. Flame 2006, 144 (4), 675–687. https://doi.org/10.1016/j.combustflame.2005.08.036.

(6) Litzinger, T.; Colket, M.; Kahandawala, M.; Katta, V.; Lee, S.-Y.; Liscinsky, D.; McNesby, K.; Pawlik, R.; Roquemore, M.; Santoro, R.; Sidhu, S.; Stouffer, S.; Wu, J. Fuel Additive Effects on Soot across a Suite of Laboratory Devices, Part 1: Ethanol. Combust. Sci. Technol. 2009, 181 (2), 310–328. https://doi.org/10.1080/00102200802437445.

(7) Kaltschmitt, M.; Streicher, W. Energie Aus Biomasse. In Regenerative Energien in Österreich; Springer, 2009; pp 339–532.

(8) Kathrotia, T.; Naumann, C.; Oßwald, P.; Köhler, M.; Riedel, U. Kinetics of Ethylene Glycol: The First Validated Reaction Scheme and First Measurements of Ignition Delay Times and Speciation Data. Combust. Flame 2017, 179, 172–184. https://doi.org/10.1016/j.combustflame.2017.01.018.

(9) Hafner, S.; Rashidi, A.; Baldea, G.; Riedel, U. A Detailed Chemical Kinetic Model of High-Temperature Ethylene Glycol Gasification. Combust. Theory Model. 2011, 15 (4), 517–535. https://doi.org/10.1080/13647830.2010.547602.

(10) Heghes, C. I. $C_1$–$C_4$ Hydrocarbon Oxidation Mechanism. PhD Diss Universität Heidelberg 2006.

(11) Marinov, N. M. A Detailed Chemical Kinetic Model for High Temperature Ethanol Oxidation. Int. J. Chem. Kinet. 1999, 31 (3), 183–220. https://doi.org/10.1002/(SICI)1097-4601(1999)31:3<183::AID-KIN3>3.0.CO;2-X.

(12) Ye, L.; Zhao, L.; Zhang, L.; Qi, F. Theoretical Studies on the Unimolecular Decomposition of Ethylene Glycol. J. Phys. Chem. A 2012, 116 (1), 55–63. https://doi.org/10.1021/jp207978n.

(13) Ye, L.; Zhang, F.; Zhang, L.; Qi, F. Theoretical Studies on the Unimolecular Decomposition of Propanediols and Glycerol. J. Phys. Chem. A 2012, 116 (18), 4457–4465. https://doi.org/10.1021/jp301424k.

(14) Hafner, S. Modellentwicklung Zur Numerischen Simulation Eines Flugstromver- Gasers Für Biomasse (Ph.D. Thesis). Universität Heidelberg 2010.

(15) Laino, T.; Tuma, C.; Moor, P.; Martin, E.; Stolz, S.; Curioni, A. Mechanisms of Propylene Glycol and Triacetin Pyrolysis. J. Phys. Chem. A 2012, 116 (18), 4602–4609. https://doi.org/10.1021/jp300997d.

(16) AlGemayel, C.; Honein, E.; Hellani, A. E.; Salman, R.; Saliba, N. A.; Shihadeh, A.; Zeaiter, J. Kinetic Modeling of the Pyrolysis of Propylene Glycol. Eng. Sci. 2022, Volume 20 (December 2022) In Progress (0).

(17) Marrodán, L.; Song, Y.; Lubrano Lavadera, M.; Herbinet, O.; de Joannon, M.; Ju, Y.; Alzueta, M. U.; Battin-Leclerc, F. Effects of Bath Gas and $NO_x$ Addition on n-Pentane Low-Temperature Oxidation in a Jet-Stirred Reactor. Energy Fuels 2019, 33 (6), 5655–5663. https://doi.org/10.1021/acs.energyfuels.9b00536.

(18) Song, Y.; Marrodán, L.; Vin, N.; Herbinet, O.; Assaf, E.; Fittschen, C.; Stagni, A.; Faravelli, T.; Alzueta, M. U.; Battin-Leclerc, F. The Sensitizing Effects of $NO_2$ and NO on Methane Low Temperature Oxidation in a Jet Stirred Reactor. Proc. Combust. Inst. 2019, 37 (1), 667–675. https://doi.org/10.1016/j.proci.2018.06.115.

(19) Pelucchi, M.; Namysl, S.; Ranzi, E.; Frassoldati, A.; Herbinet, O.; Battin-Leclerc, F.; Faravelli, T. An Experimental and Kinetic Modelling Study of n-$C_4C_6$ Aldehydes Oxidation in a Jet-Stirred Reactor. Proc. Combust. Inst. 2019, 37 (1), 389–397. https://doi.org/10.1016/j.proci.2018.07.087.

(20) Tran, L.-S.; Li, Y.; Zeng, M.; Pieper, J.; Qi, F.; Battin-Leclerc, F.; Kohse-Höinghaus, K.; Herbinet, O. Elevated Pressure Low-Temperature Oxidation of Linear Five-Heavy-Atom Fuels: Diethyl Ether, n-Pentane, and Their Mixture. Z. Für Phys. Chem. 2020, 234 (7–9), 1269–1293. https://doi.org/10.1515/zpch-2020-1613.

**TOC figure**

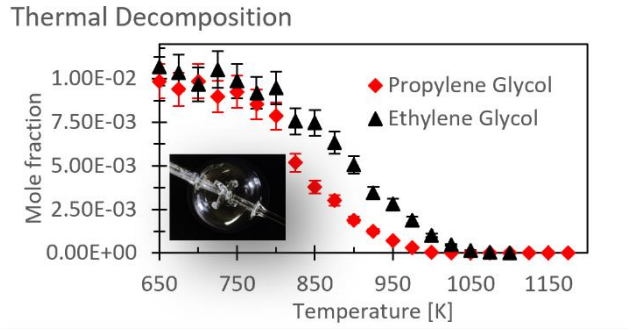
Thermal Decomposition
1.00E-02
7.50E-03
5.00E-03
2.50E-03
0.00E+00
Mole fraction
650
750
850
950
1050
1150
Temperature [K]
Propylene Glycol
Ethylene Glycol